N O T I C E

THIS DOCUMENT HAS BEEN REPRODUCED FROM MICROFICHE. ALTHOUGH IT IS RECOGNIZED THAT CERTAIN PORTIONS ARE ILLEGIBLE, IT IS BEING RELEASED IN THE INTEREST OF MAKING AVAILABLE AS MUCH INFORMATION AS POSSIBLE

9950-315

DRL No. 40
DRD No. SE-4

DOE/JPL - 954851-79/2
Distribution Category UC-63

X-Ray Measurements of Stresses and Defects in EFG and Large Grained Polycrystalline Silicon Ribbons

C. N. J. Wagner

Materials Department
School of Engineering and Applied Science
University of California
Los Angeles, CA 90024

August 1979

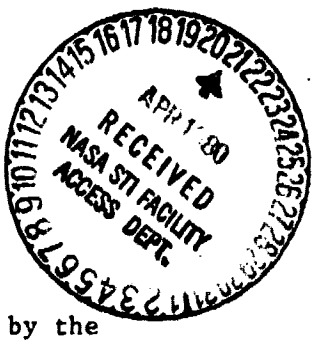

The JPL Low-Cost Silicon Solar Array Project is sponsored by the U.S. Department of Energy and forms part of the Solar Photovoltaic Conversion Program to initiate a major effort toward the development of low-cost solar arrays. This work was performed for the Jet Propulsion Laboratory, California Institute of Technology by agreement between NASA and DoE.

DISCLAIMER

SUMMARY

The Bond method has been employed to measure the lattice parameter a in an area of 0.4 mm in diameter of EFG Si-ribbons to an accuracy of ± 0.00008 Å. A Bond goniometer was built which included a goniostat with a special specimen holder to mount ribbons 1 m in length and 75 mm in width which could be rotated about two orthogonal axes, and a Leitz microscope for precision alignment of a particular area into the center of the goniostat and the small primary X-ray beam. The (321) planes were found to be parallel to the surface of the ribbons with an angular spread of about 15°. The poles of the (111) planes clustered about an angle of 25° away from the surface normal, again with a spread of 10°. The lattice parameter of a small piece of ribbon material was found to be a_o = 5.43075 A. Converting the observed strain ε (= $[a-a_o]/a_o$) into the sum of the principal surface stresses $\sigma_1 + \sigma_2$ assuming that the tilt angles of less than 15° can be neglected yielded values of $\sigma_1 + \sigma_2$ which were zero within the accuracy of our measurements of ± 10 MPa, but a maximum stress of 115 MPa was observed in a fractured ribbon which corresponded to the fracture stress of single crystals of Si.

TABLE OF CONTENTS

I. INTRODUCTION

Residual stresses are produced in EFG Si ribbons as a consequence of the growth and cooling process. These stresses might be responsible for the cracking of the ribbons during handling, processing, and service of the solar cells. Thus, the knowledge of the sign, magnitude, and distribution of these stresses would be valuable in ascertaining the severity and causes of the problem.

Built-in stresses can be readily observed by measuring the associated strains using the interplanar spacing d of crystalline materials as a strain gauge. Thus, X-ray diffraction methods can be applied for precision lattice parameter measurements in polycrystalline and single crystalline materials. In the case of silicon single crystals, the stresses are relatively small (< 15,000 psi), and, as a consequence, one must determine elastic strains $\varepsilon = \Delta d/d \sim 10^{-5}$. This can be best accomplished with a method developed by Bond [Acta Cryst. B, 814 (1960)]. A goniometer was first built based on the design of Bond which is capable of measuring $\Delta d/d \sim 10^{-5}$. We will describe briefly the principle and the construction of the Bond goniometer. Then, we give the results of the built-in strains in three EFG Si-ribbons. Attempts will be presented to correlate the measured strains with residual stresses in the ribbons.

II. TECHNICAL DISCUSSION

A. Precision Interplanar Spacing Measurements in Single Crystals

The Bond method permits the measurement of the interplanar or d-spacing to an accuracy of one part in 10^5. In this method, an X-ray detector with a large area window (e.g. 1" in diameter) is used to measure a high-angle reflection on both sides of the primary beam by rotating the single crystal from its diffraction angle $2\omega_1$ on one side of the beam to the angle $2\omega_2$ on the other side. The angle of rotation 2ω is related to the Bragg angle 2θ, i.e.,

$$2\omega = 2\omega_1 - 2\omega_2 = 180° - 2\theta \quad , \tag{1}$$

and is independent of small displacements of the sample from the axis of rotation. The angle θ can then be used to calculate the d-spacing employing Bragg's law, i.e.,

$$(2\sin\theta)/\lambda = 1/d \quad . \tag{2}$$

In order to observe a diffracted peak corresponding to a certain (hkℓ) plane in the single crystal, the Bragg-Laue equation must be satisfied, i.e.,

$$(\vec{S}-\vec{S}_o)/\lambda = \vec{H}_{hk\ell} \tag{3}$$

where $\vec{S}_o$ is the direction of the incoming X-ray beam, $\vec{S}$ is the direction of the diffracted beam, λ is the X-ray wavelength, and $\vec{H}_{hk\ell}$ is the vector normal to the reflecting planes (hkℓ), and its length is 1/d. The vector $(\vec{S}-\vec{S}_o)/\lambda$ is called the diffraction vector and its length is $2\sin\theta/\lambda$. Thus eq. (3) is the vector representation of Bragg's law [eq. (2)].

Eq. (3) requires that not only the length of the diffraction vector, i.e., $2\sin\theta/\lambda$, must be equal to the length of the reciprocal vector, i.e., $1/d$, but also that the two vectors $(\vec{S}-\vec{S}_o)/\lambda$ and $\vec{H}_{hk\ell}$ must be parallel. Thus, provision must be made to rotate $\vec{H}$ into the plane defined by $\vec{S}$ and $\vec{S}_o$, the diffraction plane, and into the direction of $(\vec{S}-\vec{S}_o)/\lambda$. This can be accomplished with a device which permits rotation about two mutually perpendicular axes, a so-called goniostat.

B. Bond Goniometer

A Bond goniometer was constructed using a 576:1 precision worm and worm gear. The angle on this goniometer can be read in number of revolutions on a 5-digit counter, and each revolution can be subdivided into 200 parts. Thus 1/100 of a revolution corresponds to 0.00625° = 22.5 sec of arc.

A goniostat (General Electric) was mounted precisely in the center of the Bond goniometer so that the ϕ axis of the goniostat at x=0 was coincident and parallel with the ω axis of the goniometer. The ϕ and x axes of the goniostat permit us to orient the single crystal in such a way that it satisfies the diffraction condition [eq. (3)].

The X-ray beam emanating from the point focus of a standard, sealed X-ray tube was collimated by two slits, one 0.3 mm in diameter close to the sample, and the other slightly larger to yield an irradiated area of 0.4 mm in diameter on the sample.

The X-ray detector (large area proportional counter:Reuter-Stokes, 2 atm. Xe gas filling, 2 inches in diameter) can be mounted alternately on

one of two dove-tail tracks, each of which could be rotated about the center of the goniometer for easy selection of the diffraction angle 2θ on either side of the primary beam slits. Utmost attention must be paid to the alignment of the primary beam (defined by the two apertures) so that it passes through the point of intersection of the two axes of rotation of the goniostat and that it is truly perpendicular to the axis of the rotation of the goniometer.

It is obvious that the reciprocal vector $\vec{H}$ must be parallel to the diffraction vector $(\vec{S}_1-\vec{S}_o)/\lambda$ and $(\vec{S}_2-\vec{S}_o)/\lambda$ which lie in the horizontal plane. Otherwise, if $\vec{H}$ is tilted by the amount δ away from the horizontal plane, the true Bragg angle θ is related to the measured angle θ' by

$$\sin\theta = \cos\delta \sin\theta' \quad . \tag{4}$$

So long as the angle of tilt δ were to remain the same in all measurements, no error would be introduced in the strain calculations since these involve only relative changes in the d-spacing.

In order to minimize δ, a horizontal, removable receiving slit has been installed in front of each detector. The width of the slit was chosen to be 1.2 mm, but can be made smaller. Since the half-widths of the crystalline Si reflections are of the order of 0.15°, we should use a slit with an opening of twice that size which corresponds to 1 mm at a crystal to detector distance of 200 mm.

A special specimen holder had to be constructed in order to mount the EFG silicon ribbon, 3 feet long and 3 inches wide, on the goniostat. It consists of a vertical dove-tail slide and a horizontal translation to locate a desired spot on the ribbon into the center of the goniostat, which could be

accurately determined with the help of a Leitz microscope. This microscope providing a very shallow depth of field and a 50X magnification was mounted on a rotatable stand directly on the goniometer table. The shallow depth of field and the cross-hair in the eyepiece of the microscope allows us to accurately position a particular area of the EFG ribbon into the X-ray beam where the d-spacing measurement is to be made.

The alignment of the Bond goniometer was checked with the aid of a narrow laser beam. In particular, it was ascertained that the diffraction plane defined by the primary beam slits and the receiving slits in front of the detector was perpendicular to the axis of rotation of the goniometer. It was determined that the crystal tilt error is limited to ± 0.14° yielding a value of $\cos\delta = 1\pm3\times10^{-6}$ which can be neglected in eq. (4) within the accuracy of the peak position determination.

In addition, a check was made of the alignment of the primary beam into the center of the goniostat. This was accomplished by aligning the tip of a fine needle into the center of rotation of the goniostat with the aid of the Leitz microscope, and by the primary beam slits so that the laser (or X-ray) beam hits the tip of the needle.

C. Precision Determination of the Position of the Diffraction Peak

Two methods have been used to determine the peak maximum position of the (444) and (642) reflections of Si employing Cu radiation, and the (440) reflection using CoKα X-rays. First, the peak profile was recorded in a slow, continuous scan (25 min/°2ω) with a digital ratemeter and a recorder.

The peak maximum was established by extrapolating the mid-cords drawn parallel to the background to the top of the peak. This method allowed us to determine $2\omega_i$ to within ± 0.005°.

In the second method, intensities were measured about the peak maximum at three or more equally spaced angular positions 2ω. The peak angle was obtained by fitting either a Gaussian curve or a parabola to the top of the peak:

(1) Gaussian Curve

$$I(2\omega) = I_{max} \exp[-(A/I_{max})(2\omega-2\omega_{max})^2]$$

where A is constant and I_{max} is the intensity at the peak maximum $2\omega_{max}$. When using 3 points at equal intervals $\Delta\omega$, the 2ω-value of the peak maximum is given by

$$2\omega_{max} = 2\omega + (\Delta 2\omega/2) + \frac{\Delta 2\omega}{1 + \frac{\ell n k_2 I_2 - \ell n k_3 I_3}{\ell n k_2 I_2 - \ell n k_1 I_1}} \qquad (5)$$

where k_i is the polarization and absorption factor

$$k_i^{-1} = [(1+1\cos\theta 1)/\sin 2\theta](1 \pm \tan\psi\cot\theta)$$

and ψ is the angle between the normal to the surface of the crystal and the normal to the reflecting planes, i.e., $\vec{H}_{hk\ell}$.

(2) Parabola

$$I(2\omega) = I_{max} - A(2\omega-2\omega_{max})^2$$

The value $2\omega_{max}$ is then given by

$$2\omega_{max} = 2\omega_1 + (\Delta 2\omega/2) + \frac{\Delta 2\omega}{1 + \frac{k_2 I_2 - k_3 I_3}{k_2 I_2 - k_1 I_1}} \qquad (6)$$

Both ratemeter and point counting methods have been used to determine $2\omega_{max}$ yielding identical results within the error of ± 0.003° in $2\omega_{max}$. According to eq. (1), the diffraction angle 2θ depends upon two peak position measurements. Consequently the error in 2ω or 2θ is ± 0.006°.

The error in the value of d-spacing can be related to the error in 2θ through Bragg's law [eq. (2)], i.e.,

$$\frac{\Delta \sin\theta}{\sin\theta} = -\frac{\Delta d}{d} = (\cot\theta)\Delta 2\theta^\circ/114.6$$

or

$$\Delta d/d = [(\tan\omega)/114.6]\Delta 2\omega^\circ = \Delta a/a \quad .$$

The error $\Delta a/a$ increases from $\pm 1\times10^{-5}$ at $\omega = 10°$ ($2\theta=160°$) to $\pm 2.5\times10^{-5}$ at $\omega = 25°$($2\theta=130°$). In the case of the (444) reflection of Si, the error in a is $\Delta a = \pm 5\times10^{-5}$ Å, and for the (642) reflection, we find $\Delta a = \pm 8\times10^{-5}$ Å .

D. Crystal Orientation and Strain Measurements in EFG Si Ribbons

At the start of this project on X-ray measurements of stresses in EFG silicon ribbons, it was assumed that the ribbons would exhibit a single crystal orientation through its length and cross-section. In all ribbons, manufactured by Mobil-Tyco and supplied by JPL, extensive variation of the crystal orientation within a single ribbon has been observed. This fact made it necessary for each measurement to reorient the ribbon in such a way that the normal $\vec{H}_{hk\ell}$ of the reflecting (hkℓ) planes, say (444), remained parallel to the diffraction vector $(\vec{S}-\vec{S}_o)/\lambda$.

Three Si ribbons have been investigated, and the crystal orientation and the lattice parameter a were determined across each ribbon at the different

locations along their length as indicated in Figs. 1-6. For each point, the lattice parameter a was evaluated from the (444) reflection using $CuK\alpha_1$ radiation (λ=1.540562 Å) and from the (642) reflection using CuKβ radiation (λ=1.392218 Å) . Because of the extensive twinning, the orientation of the reflecting planes (444) or (642) with respect to the surface of the ribbons changed considerably from point to point, but the (444) poles were clustered about angle 25° away from the surface normal with a spread of about ± 10°. Consequently, most (642) poles clustered about the center of the projection with a spread of ± 15°.

The strain-free lattice parameter a_o was determined on a small chip of the ribbon material, and was found to be a_o = 5.43075 Å. Significant changes in the lattice parameter were found only in the center row of ribbon #2, and in all rows of ribbon #3. Most other points scattered within the error bar of ± 0.00008 of these measurements about a straight line at $a = a_o$ = 5.43075 Å.

E. Residual Stresses in EFG Si Ribbons

The change in lattice parameter across and along the ribbons can be correlated with residual stresses. The state of stress at a given point in the surface of the sample is given by the principal stress σ_1 and σ_2, whose directions (called principal directions) are perpendicular to planes on which no shear stress acts. The third principal stress σ_3 normal to the surface is zero in the surface and assumed to be zero over the small depth of penetration of the X-rays into the sample surface. As long as there is no steep gradient of stress normal to the surface, this assumption will yield accurate stress values from the experimentally observed surface strains.

The strain $\epsilon_{\psi,\phi}$ in the direction, whose projection onto the specimen surface makes the angle ϕ with the direction of σ_1 and which forms the angle ψ with the normal to the surface, is given by

$$\epsilon_{\psi,\phi} = a_1^2 \epsilon_1 + a_2^2 \epsilon_2 + a_3^2 \epsilon_3 \tag{7}$$

where

$$\begin{aligned} a_1 &= \sin\psi \cos\phi \\ a_2 &= \sin\psi \sin\phi \\ a_3 &= \cos\psi \end{aligned} \tag{8}$$

and can be expressed in terms of the principal stresses σ_1 and σ_2 as

$$\epsilon_{\psi,\phi} = \frac{1}{2} S_2 \sin^2\psi(\sigma_1\cos^2\phi + \sigma_2\sin^2\phi) + S_1(\sigma_1 + \sigma_2) \tag{9}$$

where $S_1 = -\nu/E$ and $S_2/2 = (1+\nu)/E$, ν and E being Poisson's ratio and Young's modulus, respectively.

As long as the angle ψ is small, $\phi < 10°$, the first term in eq. (8) can be neglected, and the strain $(\epsilon=\Delta a/a)_{\psi<10°}$ will yield the sum of the principal stresses in Si surface, i.e.

$$\sigma_1 + \sigma_2 = \epsilon_{\psi<10°}/S_1 \quad . \tag{10}$$

The elastic constant $S_1 = -\nu/E$ can be determined from the single crystal values $s_{11} = 7.67$, $s_{12} = -2.13$, and $s_{44} = 1.27\times10^{-12}$ m^2/N, i.e.

$$S_1 = s_{12} + (s_{11}-s_{12}-s_{44}/2)\Gamma \tag{11}$$

where

$$\Gamma = (h^2k^2+k^2\ell^2+\ell^2h^2)/(h^2+k^2+\ell^2)^2 \quad .$$

The values of Γ are: $\Gamma_{111} = 1/3$ and $\Gamma_{110} = \Gamma_{321} = 1/4$ which results in values of $1/S_1$ as

$$1/S_1 = -1.025\times10^6 \text{ MN/m}^2 = -1.49\times10^5 \text{ ksi} \quad \text{for (111)}$$

and $$1/S_2 = -7.9\ 10^5 \text{ MN/m}^2 = -1.15\ 10^5 \text{ ksi} \quad \text{for (110) and (321)} .$$

For the (642) orientations, most of the measured diffraction spots satisfy the condition that the angle ψ between the specimen normal and the normal to the reflecting planes is less than 10°. This permits us to apply eq. (10). The stresses corresponding to the strain $(a-a_o)/a_o$ are also shown in Figs. 4-6. As can be readily seen, most stresses $(\sigma_1+\sigma_2)$ are less than 10 MN/m^2 = 1.45 ksi which is within the error bar of our measurements. The maximum stress is about +115 $\text{MN/m}^2 \simeq$ 17 ksi which corresponds roughly to the fracture strength of silicon.

III. CONCLUSIONS

Stresses have been determined in "single" crystal Si ribbons to an accuracy of ± 10 $MN/m^2 \simeq \pm 1.45$ ksi. This error limit can be reduced if the ribbons show a single orientation or the scatter about a single orientation is less than 5°. Because of the large mosaic structure of the Mobil-Tyco ribbon, probably produced by the extensive twinning due to the growth process (twin faults are identical to growth faults in face-centered cubic structures), the (321) planes were found to be approximately parallel to the ribbon surface with a scatter in orientation of about 15°. Fortunately, a (642) reflection could be observed using CuKβ radiation which allowed us to determine a_{321} with an error bar of ± 0.00008 Å which results in a variation of σ of ± 10 MN/m^2.

In most places where the lattice parameter could be converted to stress, i.e., where the normal to the reflecting (hkℓ) planes was within ± 15° to the normal to the surface of the Si ribbons, the sum of the principal stresses $\sigma_1 + \sigma_2$ was positive, that is tensile, with a maximum value of 115 MPa which is the fracture stress of silicon.

IV. FIGURE CAPTIONS

Figure 1 Lattice parameter a determined from the (444) reflection using $CuK\alpha_1$ radiation (λ=1.540562 Å) in different spots in ribbon #2 as indicated in the sketch.

Figure 2 Lattice parameter a determined from the (444) reflection using $CuK\alpha_1$ radiation (λ=1.5 .562 Å) in different spots in ribbon #3 as indicated in the sketch.

Figure 3 Lattice parameter a determined from the (444) reflection using $CuK\alpha_1$ radiation (λ=1.540562 Å) in different spots in ribbon #4 as indicated in the sketch.

Figure 4 Lattice parameter a determined from the (642) reflection using CuKβ radiation (λ=1.392218 Å) in different spots in ribbon #2 as indicated in the sketch. The change in lattice parameter $(a-a_o)/a_o$, where a_o=5.43075 Å, was converted into the sum of the principal stresses $\sigma_1+\sigma_2$ as indicated by the right-hand scale of the diagram.

Figure 5 Lattice parameter a determined from the (642) reflection using CuKβ radiation (λ=1.392218 Å) in different spots in ribbon #3 as indicated in the sketch. The change in lattice parameter $(a-a_o)/a_o$, where a_o=5.43075 Å, was converted into the sum of the principal stresses $\sigma_1+\sigma_2$ as indicated by the right-hand scale of the diagram.

Figure 6 Lattice parameter a determined from the (642) reflection using CuKβ radiation (λ=1.392218 Å) in different spots in ribbon #4 as indicated in the sketch. The change in lattice parameter $(a-a_o)/a_o$, where a_o=5.43075 Å, was converted into the sum of the principal stresses $\sigma_1+\sigma_2$ as indicated by the right hand scale of the diagram.

Reflection

(444)

Ribbon #2

EFG Ribbon from
Mobil Tyco Solar Energy Corp

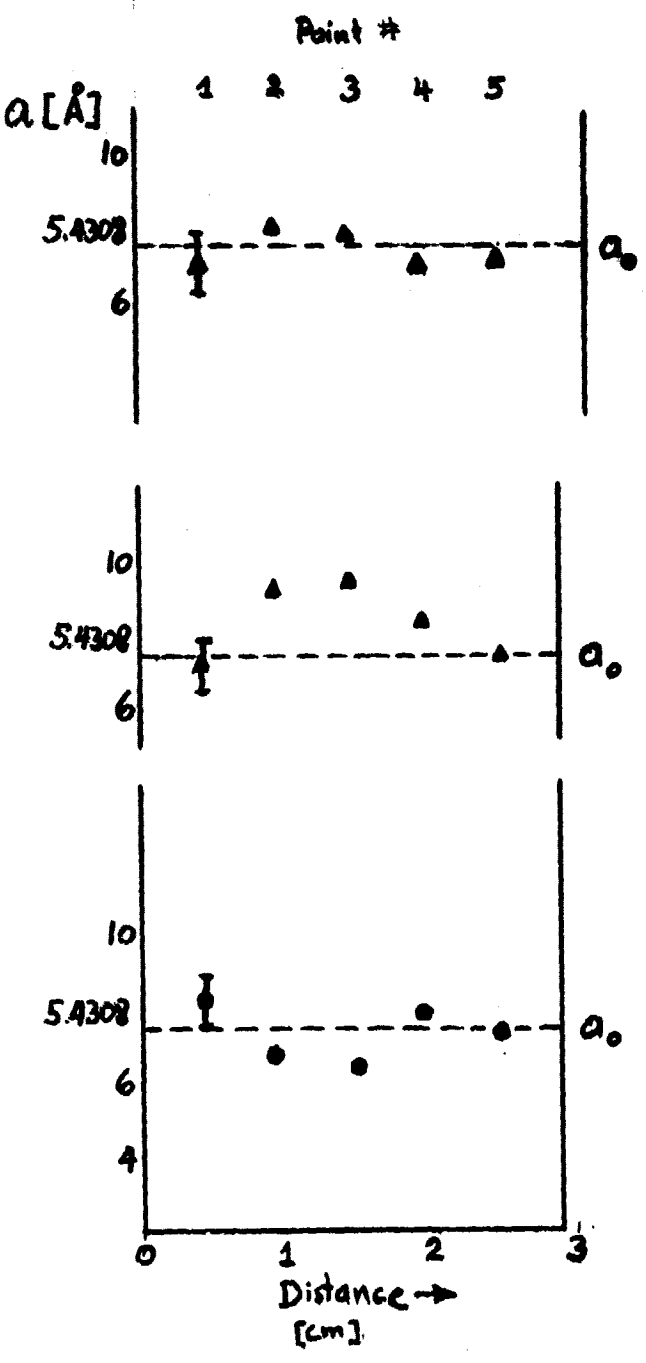

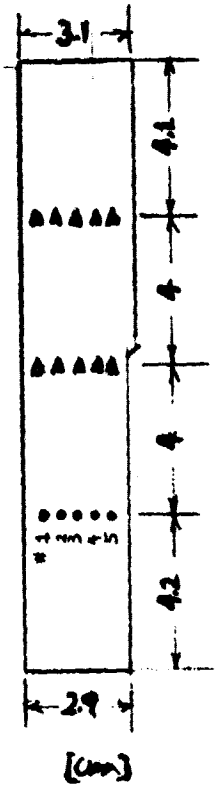

Fig 1

Reflection
(444)

Ribbon #3

JPL 5-424
Broken Section

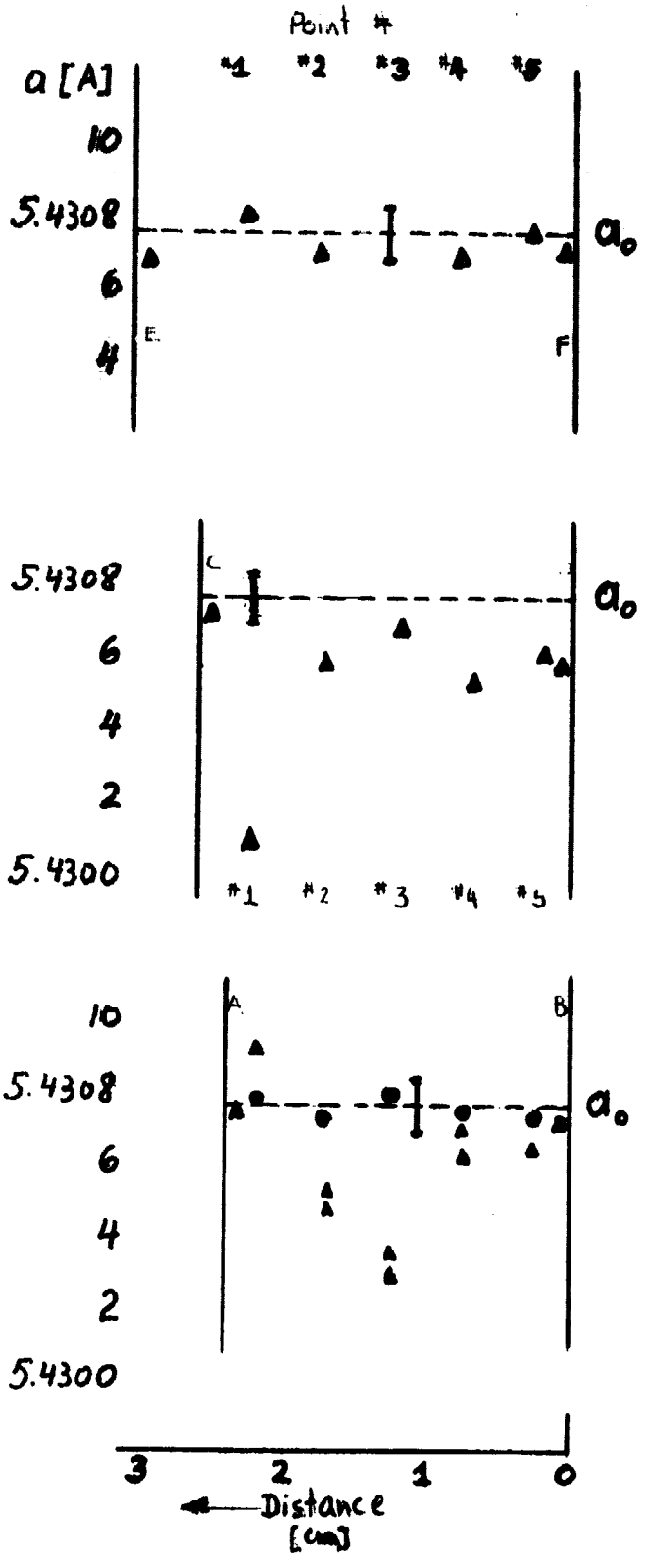

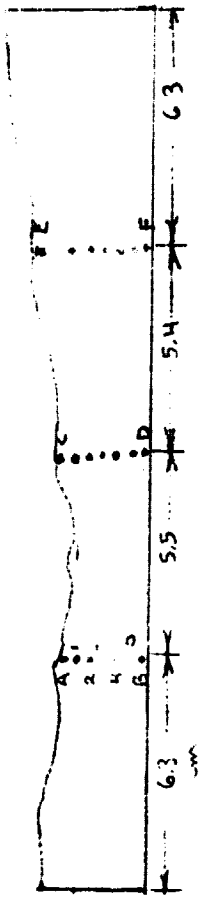

▲ 1st Run & duplications
■ x-ray beam located in approx. area.

Fig 2.

Ribbon #4

JPL 5-424

Reflection

(444)

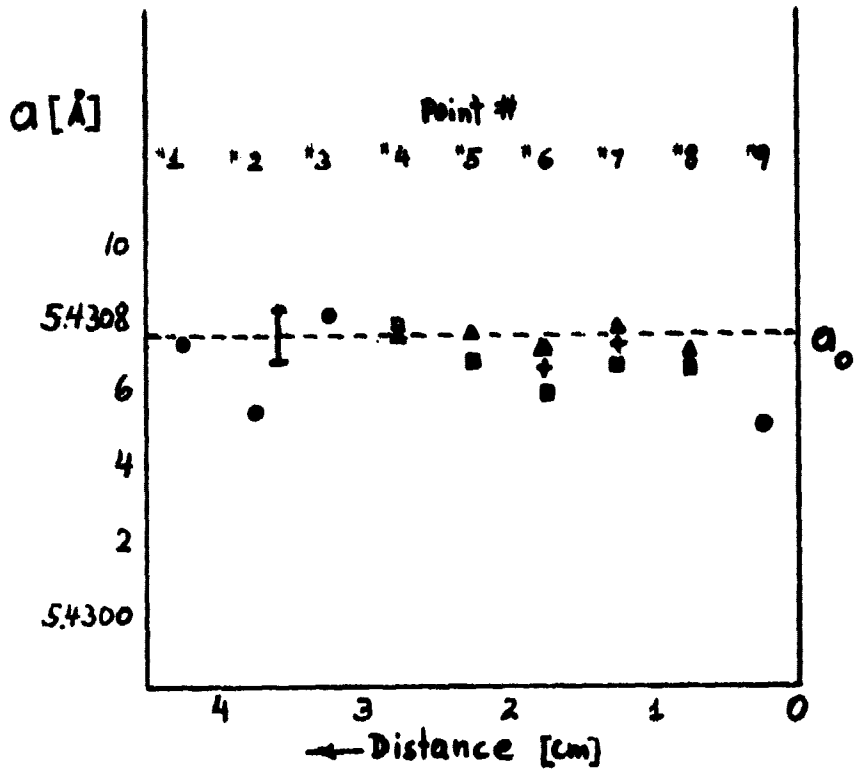

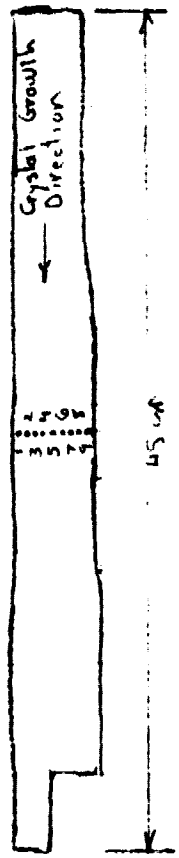

Fig. 3

Reflection
(642)

Ribbon #2

EFG Ribbon from
Mobil Tyco Solar Energy Corp.

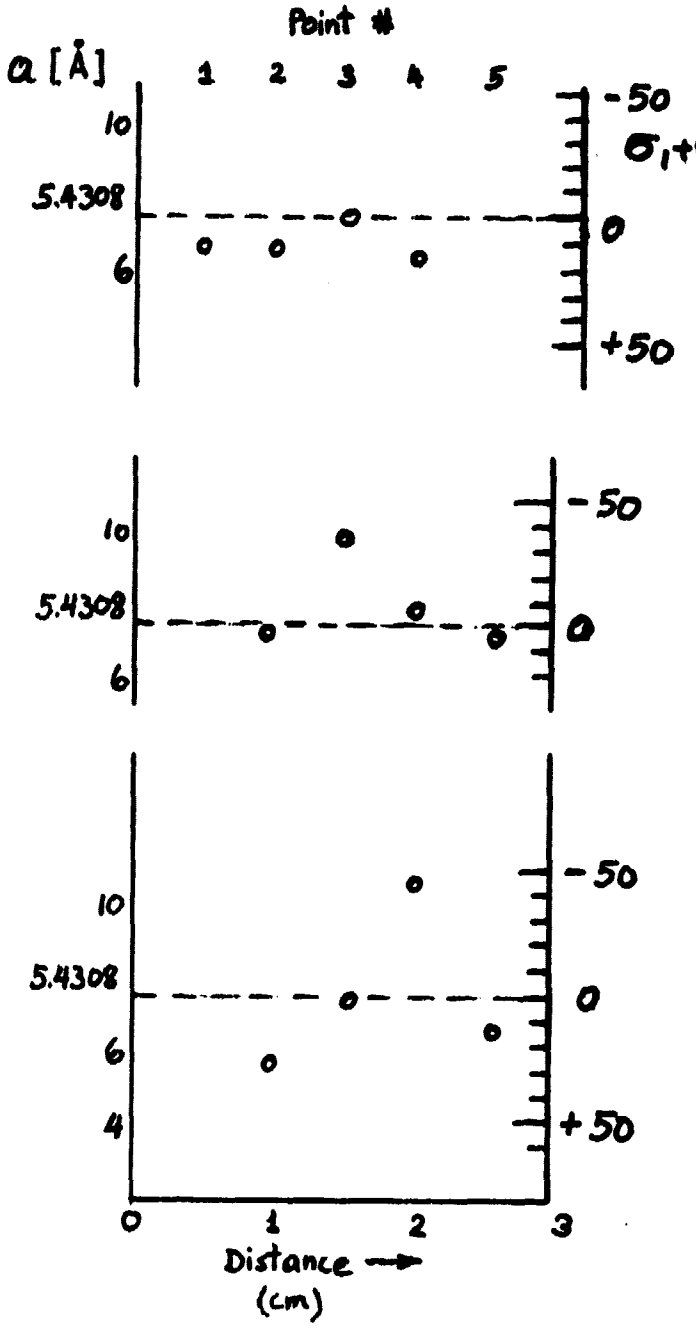

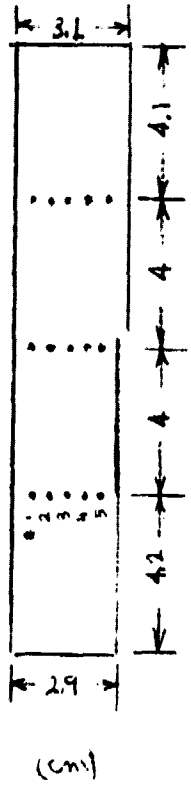

Fig. 4

Reflection
(642)

Ribbon #3

JPL 5-424
Broken Section

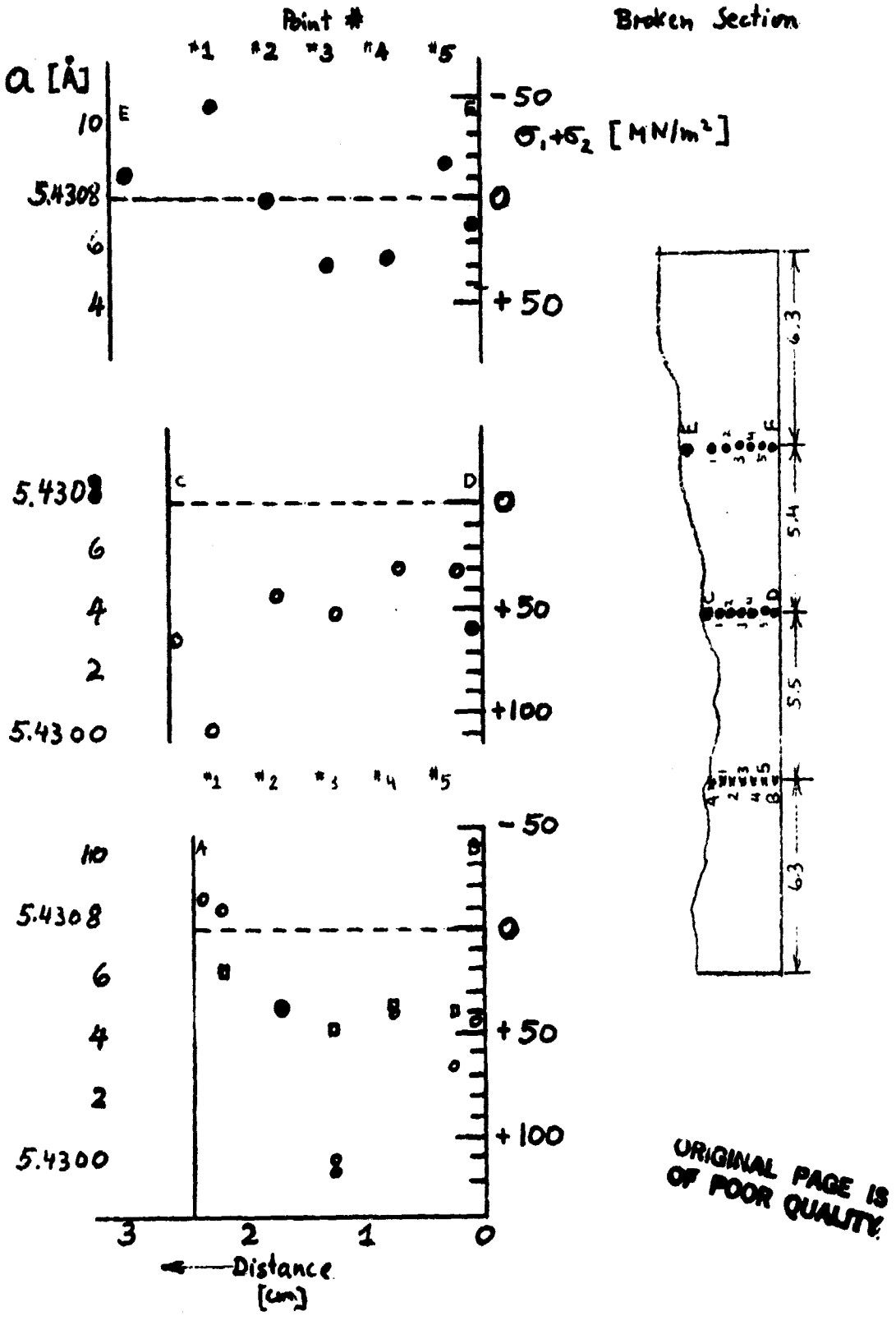

ORIGINAL PAGE IS
OF POOR QUALITY

Fig.

Ribbon #4

JPL 5-424

Reflection
(642)

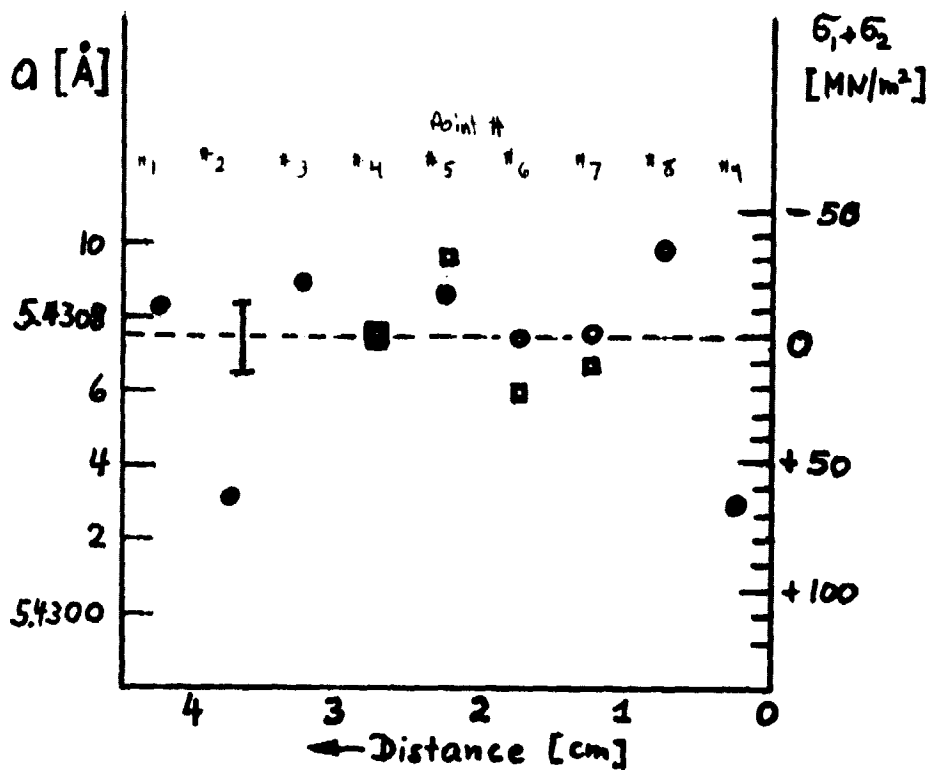

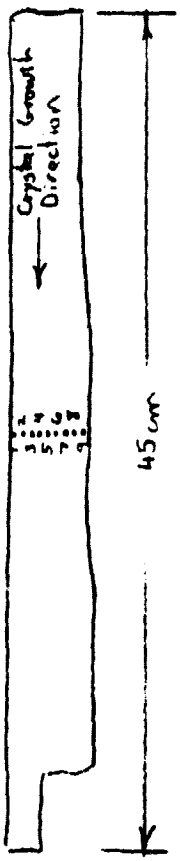

Fig. 6